

Miniaturized Drug Sensitivity and Resistance Test on Patient-Derived Cells Using Droplet-Microarray

SLAS Technology
2021, Vol. 26(3) 274–286
© Society for Laboratory
Automation and Screening 2020
DOI: 10.1177/2472630320934432
jls.sagepub.com/home/jla



Anna A. Popova¹, Sascha Dietrich^{2,3,4,5}, Wolfgang Huber^{4,5}, Markus Reischl⁶, Ravindra Peraval¹, and Pavel A. Levkin^{1,7}

Abstract

Testing the sensitivity of patient-derived tumor cells *ex vivo* can potentially help determining the appropriate treatment for each patient and spot the development of resistance to a given therapy. The number of cells obtainable from a biopsy is, however, often insufficient for performing *ex vivo* tests in conventional microtiter plates. Here, we introduce a novel Droplet-Microarray platform based on a hydrophilic-superhydrophobic patterned surface that enables screenings using only 100 cells and 30 picomoles of a drug per individual nanoliter-sized droplet. We demonstrate that the dose–response of as few as 100 primary patient-derived chronic lymphocytic leukemia (CLL) cells to anticancer compounds on the Droplet-Microarray platform resembles the dose–response obtained in 384-well plates requiring 20,000 tumor cells per experiment. The extremely miniaturized Droplet-Microarray platform thus carries great potential for *ex vivo* drug sensitivity and resistance tests on patient-derived tumor cells and potentially for implementing such tests in medical practice of precision medicine.

Keywords

drug sensitivity and resistance test (DSRT), Droplet-Microarray, drug screening, primary cells, superhydrophobicity, personalized medicine

Introduction

Cancer is the second leading cause of mortality worldwide and resulted in 8.8 million deaths worldwide in 2015.¹ Today's common practice is for cancer patients to undergo therapy without having been examined for individual sensitivities or resistance of tumor cells to certain anticancer drugs. Drug response assays were shown to be predictive of patient response *in vivo* and even though such assay needs clinical evaluation before it could be used in practice, it carries a great potential for defining a given patient's most suitable therapy. However, the amount of primary cells isolated from biopsies available for this test is not always enough. Therefore, there is a clear need for reducing cell numbers and increasing throughput per test. Here we introduce a Droplet-Microarray (DMA) platform based on a hydrophilic-superhydrophobic patterned surface that enables drug screenings using only 100 cells in individual 100 nL droplets. In this study, we report on our comparison of the drug response of primary patient-derived chronic lymphocytic leukemia (CLL) cells to anticancer compounds performed on the DMA platform and in microtiter plates.

Common anticancer drug treatment includes chemotherapy and targeted drugs that are often applied together in

¹Karlsruhe Institute of Technology, Institute of Chemical and Biological Systems, Eggenstein-Leopoldshafen, Germany

²National Center for Tumor Diseases, Heidelberg, Germany

³Medizinische Klinik V, University Hospital of Heidelberg, Heidelberg, Germany

⁴European Molecular Biology Laboratories (EMBL), Heidelberg, Germany

⁵Molecular Medicine Partnership Unit (MMPU), Heidelberg, Germany

⁶Karlsruhe Institute of Technology, Institute for Automation and Applied Informatics, Eggenstein-Leopoldshafen, Germany

⁷Karlsruhe Institute of Technology, Institute of Organic Chemistry, Karlsruhe, Germany

Received Dec 11, 2019, and in revised form March 19, 2020. Accepted for publication April 2, 2020.

Supplemental material is available online with this article.

Corresponding Authors:

Anna A. Popova, Karlsruhe Institute of Technology, Institute of Chemical and Biological Systems, Hermann-von-Helmholtz-Platz 1, Eggenstein-Leopoldshafen, 76344, Germany.
Email: anna.popova@kit.edu

Pavel A. Levkin, Karlsruhe Institute of Technology, Institute of Chemical and Biological Systems, Hermann-von-Helmholtz-Platz 1, Eggenstein-Leopoldshafen, 76344, Germany.
Email: levkin@kit.edu

so-called combinatorial drug therapy. Chemotherapeutic compounds are cytotoxic agents that are not necessarily specific to cancer cells and may also be toxic to the body's healthy cells. Targeted therapy, developed for some types of cancer, is more specific and blocks the growth of tumor cells by targeting the specific molecules involved in carcinogenesis and tumor progression² by delivering toxic agents specifically to tumor cells³ or by stimulating the immune system to attack cancer cells.⁴ Predicting which therapy a patient will most likely respond to remains a major challenge. Malignant tumors are very heterogeneous and possess high levels of intratumor (occurring in one patient) and intertumor (occurring between patients) heterogeneity. That is a reason why even the same type of tumor may respond differently to the same therapy. Methods that could help to define a given patient's individual sensitivities to a therapy before treatment include the individual molecular profiling of a tumor and the drug sensitivity and resistance test (DSRT). Molecular profiling includes collecting genomic, transcriptomic, and proteomic data from a tumor with the aim of identifying targets and biomarkers that are specific to an individual patient and predictive of that patient's response to a therapy.^{5–9} However, due to the limited number of biomarkers and incomplete understanding of the mechanism of tumor progression, it is not always possible to predict the patient response.^{10–12} Therefore, data from molecular profiling can be combined with results obtained in ex vivo DSRT, in which tumor cells obtained from a biopsy are tested against a panel of anticancer compounds for their sensitivity to different types of therapy.^{8,11,13–17} DSRT could enable the identification of drug dependencies that are not predictable via molecular profiling alone.¹¹ In addition, DSRT could allow us to repurpose existing compounds when a drug not usually prescribed for a particular cancer type is discovered to be effective against that cancer.^{8,15,16} Repeated in vitro testing of samples obtained from patients during and after the therapy could help us identify clonal selection in a tumor during treatment and identify the individual sensitivity and resistance of cancer clones. This can facilitate the therapy's adjustment to ensure the complete removal of cancer cells from the body.¹³ About 80% of trials and clinical reports on DSRT have demonstrated that it is predictive of short-term clinical responses in individual patients,^{9,13,17–24} making DSRT an important potential approach for identifying the most suitable therapy for individual patients.

DSRT is usually carried out in 96-, 384-, or 1536-well plates utilizing on average from 500 to 60,000 cells/well.^{8,13,24–26} There are about 250 approved small-molecule anticancer compounds, and enormous amount of cells would be needed to test all the available compounds and especially their combinations. As fine-needle aspiration biopsies yield on average fewer than 500,000 cells after cells have been collected for histopathological analysis,²⁷ there are no cells left for additional ex vivo sensitivity testing. In addition, as compounds and reagents are so expensive, it is critical we

lower the costs of such tests to make them affordable for each individual patient—a key factor for precision medicine. Therefore, we need highly miniaturized systems that enable the ex vivo testing of minute numbers of primary cells in small culturing volumes with large compound libraries.

We recently developed the DMA platform for cell-based screenings.^{28–31} DMA consists of an array of hydrophilic spots on superhydrophobic background. Due to the extreme difference in wettability between hydrophilic spots (water contact angle [WCA] under 10°) and superhydrophobic background (both advancing and receding WCAs exceeding 150° and sliding WCA under 5°),³² arrays of stable separated homogeneous droplets are easily formed on the planar DMA surface spontaneously either by applying aqueous solutions or by printing via nanoliter dispensers.^{29,30,33} These individual droplets can serve as miniaturized reservoirs for culturing cells. We have demonstrated the use of the DMA platform for the screening of cells of adherent^{30,33} and suspension²⁹ nature in 2D, as well as in 3D environments.^{34,35} In this paper, we have extended application of our miniaturized platform for the miniaturized DSRT on suspension primary patient-derived CLL cells. By using the DMA platform, we were able to reduce the consumption of cells by a factor of 200 compared with 384-well plates. We have validated our system with cells obtained from five different donors and nine anticancer compounds in a manual and automated setup.

Materials and Methods

Preparation of Polymer DMA Slides

Preparation of hydrophilic-superhydrophobic patterned surfaces of DMA slides has been described in detail elsewhere.^{32,33} Briefly, patterns were prepared as follows. Glass slides (Schott Nexterion, Jena, Germany) were first activated with 1 M NaOH (Carl Roth GmbH + Co. KG, Karsruhe, Germany) for 1 h, followed by neutralization with 1 M HCl (Merck KGaA, Darmstadt, Germany) for 30 min. Afterward, activated glass slides were modified with 20% v/v solution of 3-(trimethoxysilyl)propyl methacrylate (Sigma-Aldrich Chemie, Munich, Germany) in ethanol for 30 min at room temperature. A polymer layer was formed by applying 25 µL of a polymerization mixture (24 wt% 2-hydroxyethyl methacrylate [HEMA], 16 wt% ethylene dimethacrylate [EDMA], 12 wt% 1-decanol, 48 wt% cyclohexanol, and 0.4 wt% 2,2-dimethoxy-2-phenylacetophenone; all from Sigma-Aldrich Chemie) onto an inert glass slide, covering it with a modified glass slide and cross-linking the polymer by UV irradiation with a 12 mW/cm² intensity and 260 nm wavelength for 15 min. Inert glass slides were prepared by fluorination in trichloro(1H,1H,2H,2H-perfluorooctyl)silane (Sigma-Aldrich Chemie) vapor in desiccators under a 50 mbar vacuum overnight. A polymer surface was modified with alkyne groups by incubating the

Table I. Comparison of Workflows and Consumptions of Compounds, Cells, and Reagents of Screening Performed on the DMA Platform and in 384-Well Plates.

Screening Workflow	Consumption per Droplet/Well	Droplet-Microarray	384-Well Plate
Dispensing compounds	Compounds	0.03 nmol	10 nmol
Seeding cells	Cells	100	20,000
Screening initiation		Sandwiching (manual setup) During seeding (automated setup)	During seeding
Incubation for 48 h		Yes	
Readout assay	Reagents	Live/dead staining 50 nL	CellTiter-Glo assay 25,000 nL
Readout		Microscopy	Luminescence measurement

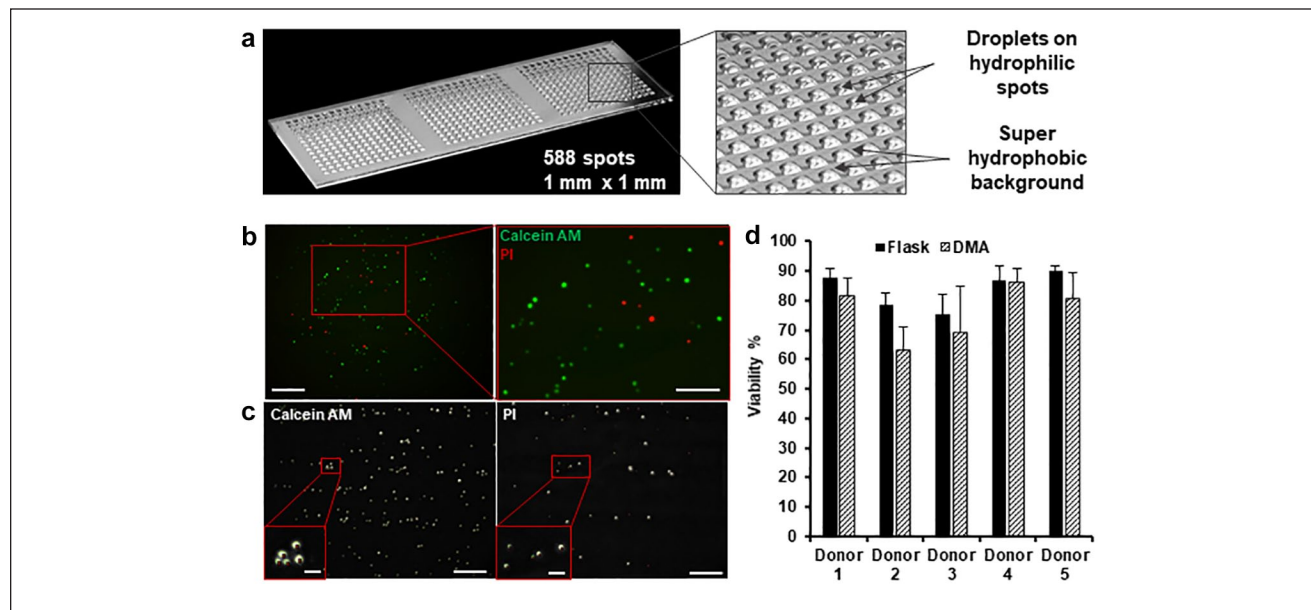


Figure 1. The DMA platform. (a) A photograph of a nonpolymer DMA slide containing droplets of water. The photo was taken by the team from the Crossmedia department of KIT (photo: Amadeus Bramsiepe; head of department: Dipl. Inf. Willi Mueller). (b) Microscope images of primary CLL cells incubated on polymer DMA for 48 h and stained with calcein AM and PI. Scale bars = 100 μ m, insert 50 μ m. (c) Microscope images showing cell count using in-house developed algorithm. Scale bars = 100 μ m, insert 20 μ m. (d) Graph showing comparison of viability of CLL cells isolated from five different donors and cultured on polymer DMA slides (black bars) and in cell culture flask (dotted bars) for 48 h.

slides in solution containing 45 mL of dichloromethane (Merck KGaA), 56 mg of 4-(dimethylamino)pyridine (Novabiochem, Merck KGaA), 111.6 mg of pentynoic acid (Sigma-Aldrich Chemie), and 180 μ L of *N,N'*-diisopropylcarbodiimide (Alfa Aesar GmbH & Co KG, Karlsruhe, Germany) for 4 h under stirring at room temperature. A superhydrophobic background was created by applying a 5% v/v solution of 1*H*,1*H*,2*H*,2*H*-perfluorodecanethiol (Sigma-Aldrich Chemie) in acetone onto the polymer surface and irradiating the slide through a photomask (Rose fotomasken, Bergisch Gladbach, Germany) with 260 nm of UV light at 12 mW/cm² for 1 min. Afterward, hydrophilic spots were created by applying 10% v/v β -mercaptoethanol

(Alfa Aesar) solution in 1:1 water–ethanol onto the patterned surface and irradiating the slide with 260 nm of UV light at 12 mW/cm² for 1 min.

Printing of Compounds

Anticancer compounds in different concentrations and four repeats per each concentration were printed onto hydrophobic glass slides or directly to hydrophilic spots of polymer or nonpolymer DMA. Hydrophobic glass slides were prepared as follows. Microscope glass slides (Schott Nexterion, Jena, Germany) were fluorinated by trichloro(1*H*,1*H*,2*H*,2*H*-perfluoroctyl)silane (Sigma-Aldrich, Chemie) under a

50 mbar vacuum in a sealed desiccator containing an open vial of the silane overnight. Frozen aliquots of antineoplastic compounds in DMSO were provided by Molecular Therapy in Hematology and Oncology, and the Department of Translational Oncology, National Center for Tumor Diseases and German Cancer Research Centre, Heidelberg, Germany and are listed in **Supplemental Table S1**. Compounds were obtained from Sigma-Aldrich Chemie, Enzo Life Sciences, Selleck Chemicals, and Merck and were dissolved in DMSO at 0.1–50 mM (mainly 10 mM) and stored at –20 °C.⁸ Compounds were diluted in pure RPMI-1640 medium (Gibco, Life Technologies GmbH, Darmstadt, Germany) and printed in different amounts using the sciFLEXARRAYER S11 liquid dispenser (Scienion, Berlin, Germany) to ensure the following final concentrations in droplets: 0.041, 0.123, 0.37, 1, 3, 10, 30, 50, 100, and 200 μM. The final concentration of compounds was calculated for final volumes of 80 and 100 nL for manual and automated seeding, respectively. For the manual sandwiching method, 4 replicates were used for each concentration, and 20 replicates for the control. For automated setup, four repetitions were used for each concentration and the control. After printing, slides containing preprinted compounds were incubated in the Schlenk line (vacuum gas manifold) for at least 1 h in order to evaporate DMSO content from preprinted spots. Afterward, preprinted slides were stored in a dark box containing silica gel (Sigma-Aldrich Chemie) before use.

Primary CLL Cells

Peripheral blood samples from five leukemia and lymphoma patients were obtained from Molecular Therapy in Hematology and Oncology, and the Department of Translational Oncology, National Center for Tumor Diseases and German Cancer Research Centre, Heidelberg, Germany. Blood was separated by a Ficoll gradient (GE Healthcare, Munich, Germany), and mononuclear cells were cryopreserved.⁸ All procedures for obtaining and preserving patient-derived cells were approved by the Ethics Committee Heidelberg (University of Heidelberg, Germany; S-356/2013).

Culturing Cells on DMA Platform

Jurkat human T-cell lymphocyte cells were cultured in RPMI-1640 medium (Gibco, Life Technologies) supplemented with 10% heat-inactivated fetal bovine serum (FBS; Sigma-Aldrich Chemie) and 1% penicillin/streptomycin (Gibco, Life Technologies). Cells were cultured in T25 flasks and diluted every 2–3 days until a cell density of 2×10^5 cells/mL was achieved.

Primary patient-derived CLL cells were obtained from National Center for Tumor Diseases, Heidelberg, Germany. CLL cells were isolated and frozen as described in the

“Isolation of Primary CLL Cells” section. CLL cells were thawed by placing the vial containing cells in a 37 °C water bath for a few seconds before most of the liquid was thawed and only small ice clumps were still left. Cells were resuspended in 10 mL of RPMI-1640 medium (Gibco, Life Technologies) supplemented with 10% heat-inactivated FBS (Sigma-Aldrich Chemie) and 1% penicillin/streptomycin (Gibco, Life Technologies). Afterward, cells were centrifuged with 1000 rpm for 5 min. Supernatant was removed and cell pellet was resuspended in 10 mL of RPMI-1640 medium (Gibco, Life Technologies) supplemented with 15% heat-inactivated AB-type human serum (RPMI-HS, MP Biomedicals), 1% glutamine (Invitrogen), and 1% penicillin/streptomycin (Gibco, Life Technologies). Cells were counted with the automated cell counter Countess II FL (Thermo Fisher Scientific Inc., Darmstadt, Germany) and diluted to a desired cell concentration.

Cells were seeded on polymer or nonpolymer DMA slides. Polymer DMA slides were prepared as described in the “Preparation of Polymer DMA Slides” section and preconditioned before cell culture as follows. First, DMA slides were sterilized by immersion in 100% ethanol, followed by drying under a sterile bench for at least 20 min before use. Afterward, DMA slides were coated with 2.2% bovine gelatin (Sigma-Aldrich Chemie) in RPMI medium containing 1% heat-inactivated FBS (Sigma-Aldrich Chemie) and 1% penicillin/streptomycin (Gibco, Life Technologies). Coating was done manually by rolling the droplet of gelatin across the array, resulting in spontaneous droplet formation. Afterward, slides were incubated in a cell culture incubator for 1 h and dried for 20 min under a sterile bench before use. Nonpolymer DMA slides were obtained from Aquarray GmbH (Eggenstein-Leopoldshafen, Germany). Slides were sterilized by immersion in 100% ethanol, followed by drying under a sterile bench for at least 20 min before use. Afterward, nonpolymer DMA slides were either directly used for cell seeding or coated with gelatin as described above for polymer DMA.

Both CLL and Jurkat cells were seeded on DMA slides either manually, using the effect of spontaneous droplet formation, or with an I-DOT nanoliter dispenser (Dispendix GmbH, Stuttgart, Germany). For manual seeding, cells were diluted to a final concentration of 75×10^4 cells/mL. A preconditioned DMA slide was placed into a petri dish. Cells were seeded by applying 1.7 mL of cell suspension onto one array field containing 14×14 spots (total 196) and a petri dish was closed with a humidifying lid, which contained a cloth pad wetted with buffer. Cell suspension was incubated on the DMA slide for 90 s, followed by slight (~45°) tilting of the petri dish with the DMA slide to allow for the spontaneous formation of an array of droplets containing cells. Afterward, a petri dish with the DMA slide was placed in a cell culture incubator. For seeding with I-DOT nanoliter dispenser cells were diluted to a final concentration of 100×10^4 cells/mL and dispensed directly to

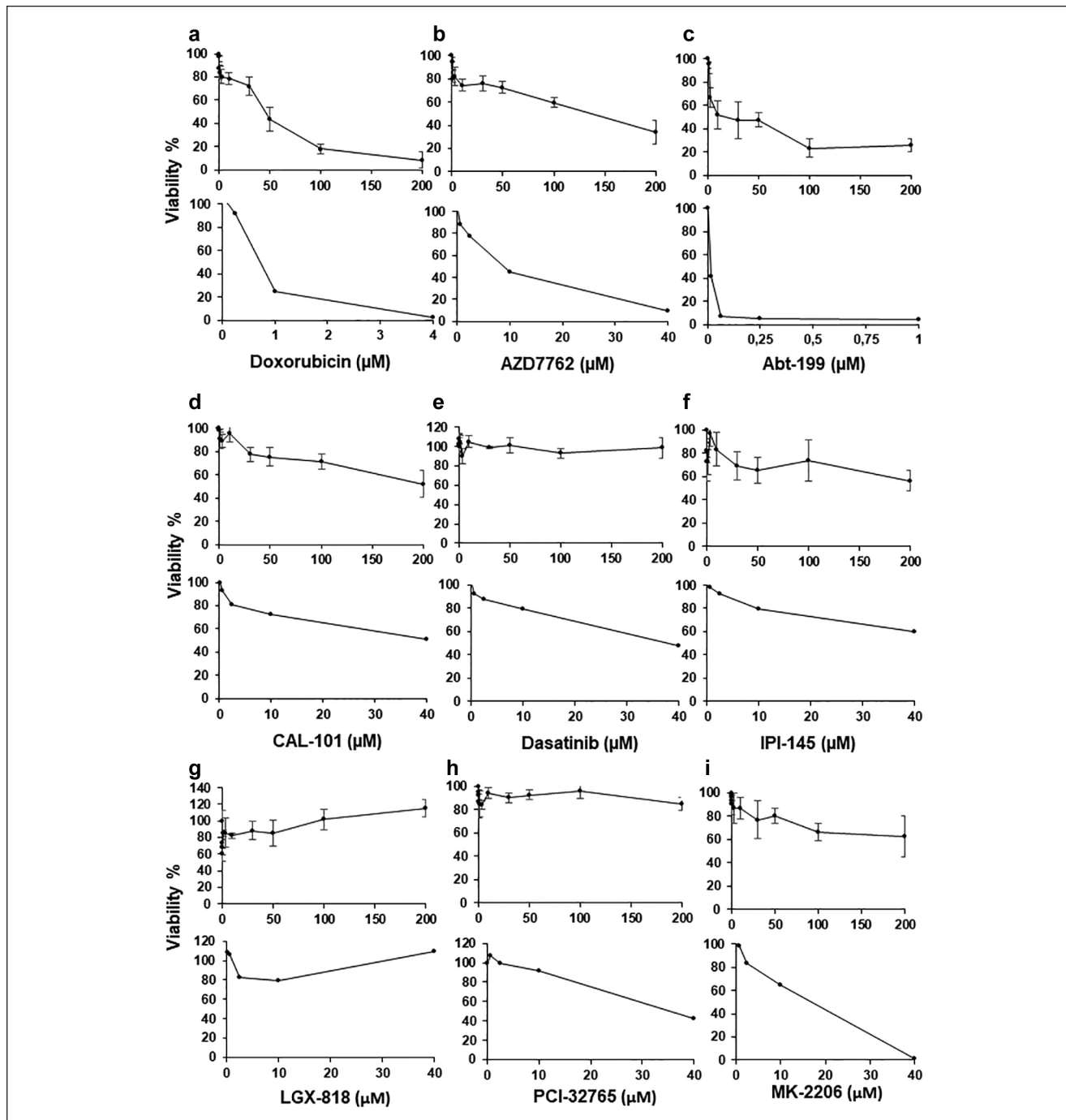


Figure 2. Comparison of dose-dependent effects of compounds on primary patient-derived CLL cells isolated from donor I on the polymer DMA platform (upper panel) and 384-well plate (lower panel): (a) doxorubicin, (b) AZD7762, (c) Abt-199, (d) CAL-101, (e) dasatinib, (f) IPI-145, (g) LGX-818, (h) PCI-32765, and (i) MK-2206. In case of the DMA platform, the average was taken from four repeats; error bars are standard deviations. In the case of the 384-well plate, we did only one repeat per concentration. It should be noted that the scales for the x axis are different for DMA and 384-well plates.

hydrophilic spots in a 100 nL volume obtaining on average 100 cells/spot. Afterward, the DMA slide containing cells was placed into a petri dish with a humidified lid and placed in a cell culture incubator.

All experimental protocols performed with patient-derived cells were approved by the Ethics Committee Heidelberg (University of Heidelberg, Germany; S-356/2013).

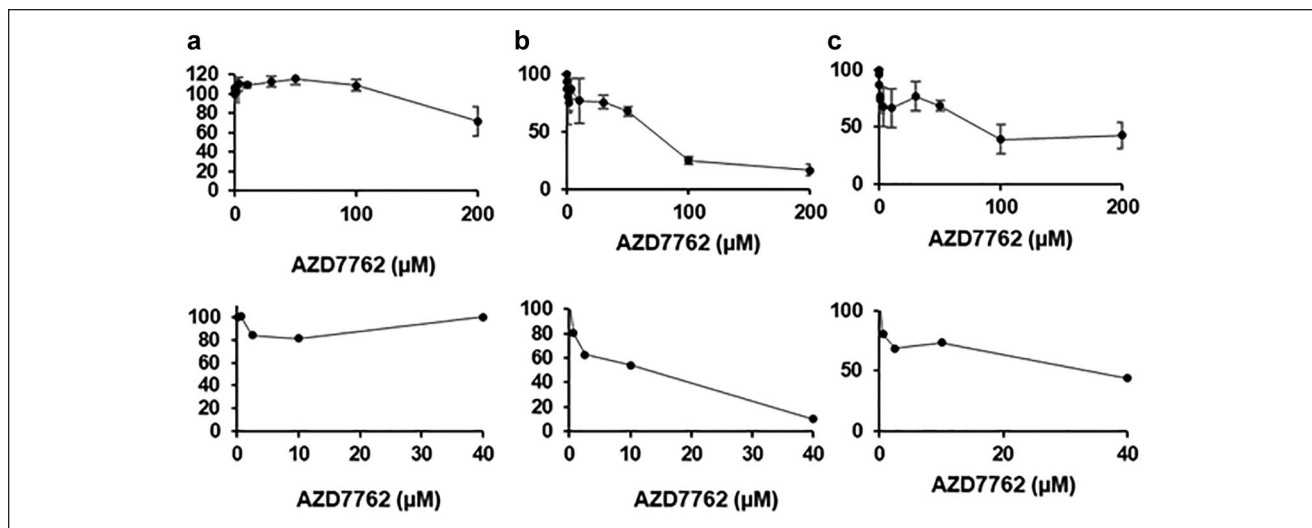


Figure 3. Comparison of dose-dependent effects of compounds on primary patient-derived CLL cells isolated from three different donors on the polymer DMA platform with manual setup (upper panel) and 384-well plate (lower panel): (a) donor 3, (b) donor 4, and (c) donor 5. In the case of the DMA platform, the average was taken from four repeats; error bars are standard deviations. In the case of the 384-well plate, we did only one repeat per concentration. It should be noted that the scales for the x axis are different for DMA and 384-well plates.

Manual DSRT on DMA Platform

The range of compound concentrations (four repeats per each concentration) were printed as described in the “Printing of Compounds” section. Cells were thawed and seeded manually as described in the “Culturing Cells on DMA Platform” section. After seeding, cells were incubated in a cell culture incubator for 2 h prior to introduction to compounds. Compounds were introduced to cells using the sandwiching method and aligning the frame, as described previously (Suppl. Fig. S1).²⁹ Glass slide containing compounds were fixed in the upper holder of the aligner. The DMA slide with cells was fixed in the lower holder of the aligner (Suppl. Fig. S1). The aligner was closed and the upper glass slide with compounds brought down gradually in a parallel manner by turning adjusting screws counterclockwise (Suppl. Fig. S1, red arrows) before the droplets touched the glass surface, which was visually observed in the aligner window (Suppl. Fig. S1). Afterward, the aligner frame was placed in a cell culture incubator for 15 min. To avoid evaporation during the sandwiching step, the aligner was placed in a tray and covered with sterile paper tissues wetted with sterile buffer. To open the aligner, four screws controlling the distance between the slides (Suppl. Fig. S1, red arrows) were turned clockwise until the droplets were no longer in contact. After opening that frame, the DMA slide containing cells was returned to a petri dish with a humidified lid and put in a cell culture incubator. Cells were incubated for 48 h with compounds before the readout assay was done. For the readout assay, cells were stained with calcein AM (Thermo Scientific,

Waltham, MA) and PI (Invitrogen, Merelbeke, Belgium) via the sandwiching method. For this, solution containing 50 μ g/mL calcein AM and 50 μ g/mL PI in phosphate-buffered saline (PBS; Gibco, Life Technologies) was spread on an empty polymer DMA slide by rolling the droplet of solution across the patterned surface, resulting in the formation of an array of droplets. A DMA slide with staining solution was sandwiched with the DMA slide containing cells as described above. Cells were incubated in a closed aligner for 15 min in a cell culture incubator in a humid environment. Afterward, the aligner was opened and the DMA slide containing stained cells was placed in a four-well dish (Thermo Scientific Nunc) and imaged using an automated screening Olympus IX81 microscope (Tokyo, Japan).

Imaging and Image Analysis

Imaging was performed using an automated screening Olympus IX81 microscope. The grid of the DMA pattern was defined in the microscope software. The autofocus function “interpolate AF” was used to minimize defects that can arise from uneven surface thickness and unparalleled slide positioning. Z stacks of 10 slices were made to obtain cells in focus as suspension cells are on slightly different focal planes. The images of one central field of view per each SL spot were taken at 10 \times magnification in three different channels: bright field, GFP (for calcein AM), and RFP (for PI). For analysis, images obtained from 10 Z stacks were merged using the “Extended Depth” algorithm in ImageJ software (NIH, Bethesda, MD). Numbers of calcein AM and PI-positive cells were calculated using a

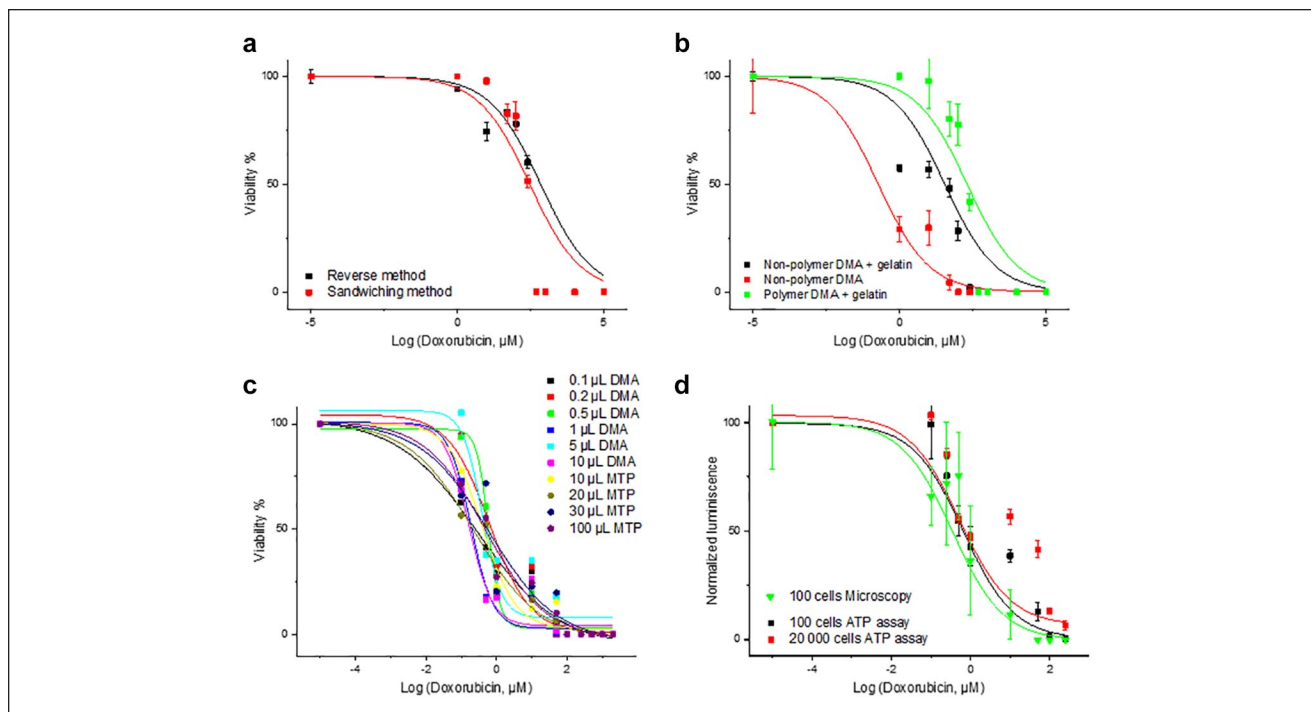


Figure 4. Comparison of dose-dependent effects of doxorubicin on Jurkat cells on nonpolymer DMA using different experimental setups: (a) comparison of reverse and sandwiching methods of compound introduction, (b) comparison of different surfaces, (c) comparison of different culturing volumes ranging from 0.1 to 100 μ L, and (d) comparison of different readouts: microscopy based (red) and fluorescent based (black) with 100 and 20,000 cells/well.

specially developed algorithm for the automated counting of cells described previously.²⁹

Estimation of Cell Viability in Flask

The viability of cells cultured in flasks was estimated by two different methods. In the first method, an aliquot of cell suspension from the flask was stained with Trypan blue and cells were counted in a Countess II FL cell counting machine. In the second method, the cells cultured in flask were seeded on an empty DMA slide and cells were immediately stained with calcein AM/PI using the sandwiching method, followed by imaging. Both methods to estimate viability in the control flask yielded similar results.

Automated DSRT on DMA Platform

Nonpolymer DMA slides were purchased from Aquarray. The range of compound concentrations was printed directly into hydrophilic spots as described in the “Printing of Compounds” section. Cells were thawed and seeded using an I-DOT dispenser (Dispendix) as described in the “Culturing Cells on DMA Platform” section. Cells were incubated for 48 h with compounds before doing the readout assay. For the readout assay, cells were stained with calcein AM (Thermo Scientific) and PI (Invitrogen) by

dispensing 50 nL of staining solution (1.5 μ g/mL calcein AM and 3 μ g/mL PI in PBS) directly into each droplet and incubating for 15 min in the cell culture incubator. Cell imaging and image analysis took place as described in the “Manual DSRT on DMA Platform” section.

Obtaining Dose-Dependent Curves in Different Volumes

Compound doxorubicin in water was printed with an I-DOT dispenser (Dispendix) directly in hydrophilic spots of nonpolymer, noncoated DMA slides or in wells of microtiter plates in different amounts to ensure the following range of final concentrations in each volume tested: 0.041, 0.123, 0.37, 1, 3, 10, 30, 50, 100, and 200 μ M. Afterward, the Jurkat cells were seeded in 100 cells/spot or cells/well in volumes ranging from 0.1 to 100 μ L using an I-DOT dispenser (Dispendix) either on nonpolymer, noncoated DMA slides or in microtiter plates. To obtain 100 cells in each volume, several cell dilutions were done to ensure an average of 100 cells per each volume tested. Volumes 0.1 and 0.2 μ L were tested on DMA slides with spot sizes 1 \times 1 mm; volumes 0.5 and 1 μ L on DMA slides with spot sizes 1.4 \times 1.4 mm; volumes 5 and 10 μ L on DMA slides with spot sizes 3 \times 3 mm; volumes 10, 20, and 30 μ L in a 384-well plate; and volume 100 μ L in a 96-well plate (Fig. 4c). Cells

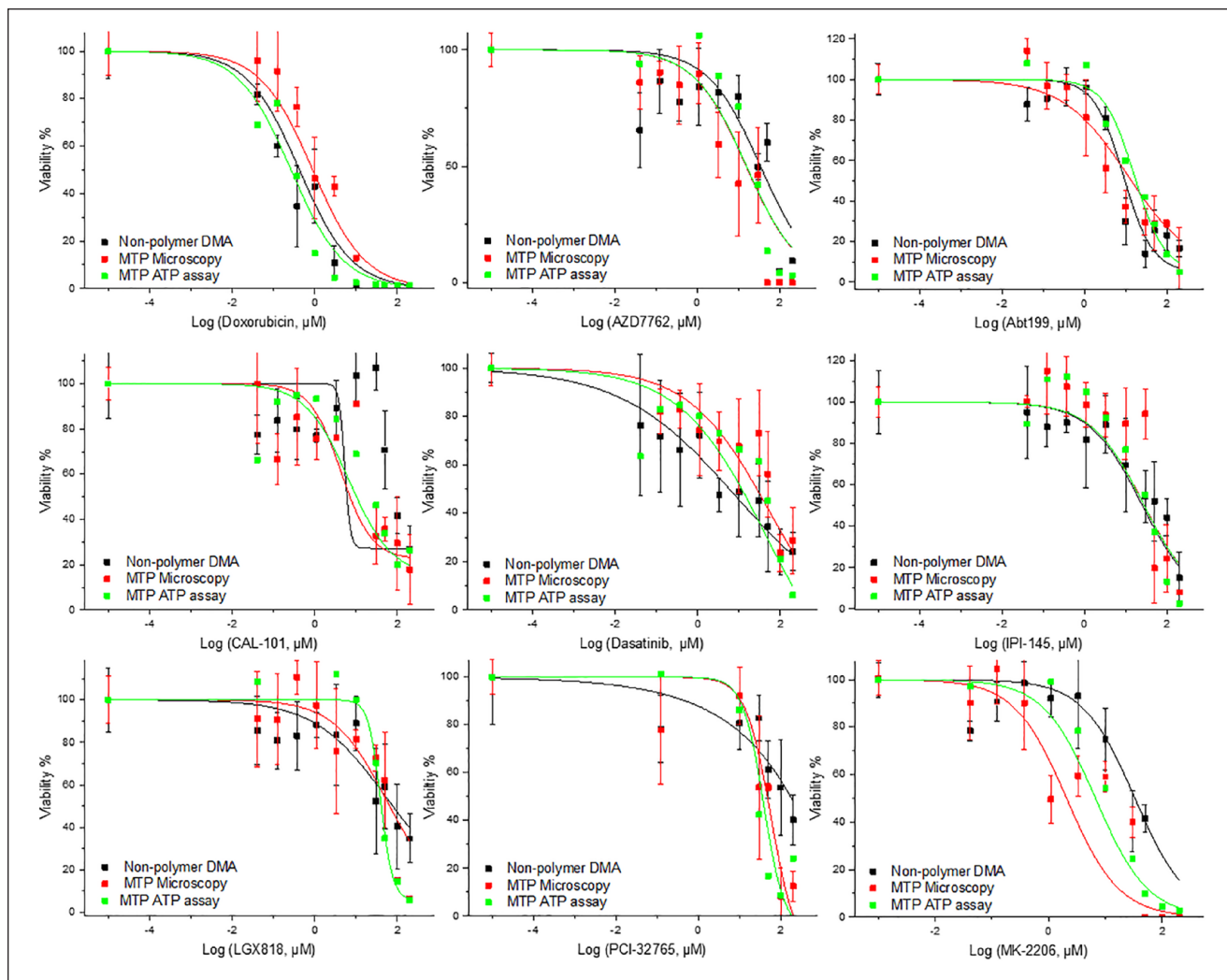


Figure 5. Comparison of dose-dependent effects of compounds on primary patient-derived CLL cells on nonpolymer DMA and in a 384-well plate using microscopy- and luminescence-based readouts. All experiments were performed on cells isolated from donor 4, except for the dose-dependent effect of Abt199, which was performed on cells from donor 2. In the case of the DMA platform, the average was taken from four repeats; error bars are standard deviations. In the case of a 384-well plate, the microscopy-based readout average was taken from three repeats; error bars are standard deviations. In the case of a 384-well plate luminescence-based readout, only one repeat per concentration was made.

were incubated for 48 h with compounds. For the readout assay, cells were stained by dispensing staining solution containing calcein AM (Thermo Scientific) and PI (Invitrogen) into spots or wells using an I-DOT dispenser. The staining solution's amount and concentration were adjusted to ensure the following final dye concentrations: 0.5 μ g/mL calcein AM and 1 μ g/mL PI. Cells were incubated for 15 min in the cell culture incubator and subjected to imaging using an automated screening Olympus IX81 microscope or Keyence BZ-9000 (Osaka, Japan). Images were taken at 4 \times magnification in three different channels: bright field, GFP (for calcein AM), and RFP (for PI). The amount of calcein AM and PI positive cells was counted using ImageJ software.

CellTiter Glo Assay in 384-Well Plate

Cells were seeded in amounts of 100 or 20,000 cells/well in 30 μ L of medium in wells preprinted with compounds. After 48 h of incubation with compounds, 30 μ L of CellTiter Glo reagent (Promega, Madison, WI) was added to each well, and the plate was shaken for 2 min and incubated for 30 min. Luminescence was then measured using a 1420 Luminescence Counter Victor Light (PerkinElmer, Waltham, MA) and integration time of 2 s/well.

Statistical Analysis

Error bars on all published graphs represent standard deviations.

Dose-response curves in **Figures 4 and 5** were plotted in OriginPro using “Nonlinear curve fit,” category “Growth/Sigmoidal,” function “DoseResp,” iteration algorithm “Levenberg Marquardt,” and multidata fit mode “Independent fit.” IC₅₀ values were calculated in OriginPro after curve fitting.

The Z' factor was calculated using DMSO as a negative control and doxorubicin treatment as a positive control. The following formula was used: $Z' \text{ factor} = 1 - (3 * (\sigma_0 + \sigma_{\text{Dox}}) / (\mu_0 - \mu_{\text{Dox}}))$, where σ_0 is the standard deviation of viabilities of control, σ_{Dox} is the standard deviation of viabilities of cells after treatment with doxorubicin at a concentration of 10 μM for nonpolymer and 200 μM for polymer DMAs, μ_0 is the average viabilities of the control, and $\mu_{\text{Dox}10}$ is the average viabilities of cells treated with doxorubicin at a concentration of 10 μM for nonpolymer and 200 μM for polymer DMAs.

Results and Discussion

Workflow of DSRT on the DMA Platform Using a Manual Setup

The workflow of a miniaturized DSRT and its step-by-step comparison with a workflow used in 384-well plates is presented in **Table 1**. For the miniaturized DSRT using the manual setup, we used DMA slides^{29–31,33,34,36} with a polymer surface coating, manufactured by coating standard glass slides (7.5 \times 2.5 cm) with a thin layer of rough and porous methacrylate-based polymer, followed by selectively modified hydrophilic and superhydrophobic areas with hydrophilic and hydrophobic chemical groups, respectively (see Materials and Methods). The array grid's design was defined by a photomask and was precisely controllable. In the current study, we used DMAs containing 588 square hydrophilic spots with a side length of 1 mm capable of trapping about 80 nL of volume (**Fig. 1a**).^{29,33}

Primary patient-derived CLL cells were seeded on DMAs by applying cell suspension onto the polymer surface to cover the whole array of spots followed by tilting the DMA slide, which resulted in spontaneous formation of an array of separated droplets containing cells (**Fig. 1a**).^{29,33} This technique allowed us to form an array of 588 droplets with cells simultaneously within seconds without having to pipette each individual droplet. Anticancer compounds (**Suppl. Table S1**) were added to the cells on DMA via the sandwiching method established by us previously.^{29,30} For this, we first printed compounds in different concentrations onto a fluorinated glass slide in a geometric pattern corresponding to the pattern of hydrophilic spots on DMA slides and then dried them. Afterward, we sandwiched the compound array slide with the DMA slide containing cells using a manual sandwiching frame (**Suppl. Fig. S1**), bringing each droplet with cells in contact with the preprinted

compound for 15 min.²⁹ We have demonstrated previously that the transfer rate for substances dissolved in both water and DMSO is nearly 100% using this protocol for sandwiching.³⁰ After opening the sandwiching frame, the DMA slide with cells was incubated with anticancer compounds in an incubator for 48 h. To avoid evaporation, DMAs were placed into a semiclosed chamber with controlled humidity. To estimate cell viability, we stained cells with calcein AM and propidium iodide (PI) by applying the manual sandwiching approach. For this, we first spread staining solution onto an empty DMA slide utilizing the ability of spontaneous droplet formation, and then added the staining solution to the cells by sandwiching the DMA slide containing cells with that containing staining solution as described before for compound addition.²⁹ The cells were imaged using an automated screening fluorescence microscope; our results are illustrated in **Figure 1b**.²⁹

The cell screening workflow based on our DMA platform has several advantages over the state-of-the-art microtiter plates. First, the same screen done in 384-well plates required 200 times more cells (20,000 vs 100), 300 times more compounds (10 nmol vs 0.03 nmol), and 500 times more reagents (25,000 nL vs 50 nL) per each well (**Table 1**). Second, the DMA platform does not necessarily require expensive equipment and can be used manually, which requires neither multiple pipetting steps nor liquid handling automation. When provided with DMAs containing a compound library, laboratories not equipped with liquid handling robotics can perform cell screenings manually without a need for additional expensive machinery.

Culturing Primary Patient-Derived CLL Cells Using the DMA Platform

In the present study, we used primary patient-derived CLL cells from frozen peripheral blood samples. Blood samples were obtained from five leukemia and lymphoma patients and provided by the University Hospital Heidelberg. CLL cells do not proliferate in vitro or in the blood. We have stained CLL cells cultured in 384-well plates for Ki-67, a proliferation marker, which showed that less than 1% of cells were proliferating (**Suppl. Fig. S4**). Chemotherapy interferes with spontaneous DNA repair mechanisms, induces p53, and thereby induces apoptosis. Previously, we showed that CLL cell cultured in vitro upregulated p53 after DNA damage, which finally lead to apoptosis, even though these cells were nonproliferating. We have also compared cell response after 48 and 72 h of incubation and did not observe a significant difference.⁸ After 48 h incubation with drugs in vitro, a significant spontaneous cell death in response to drugs was observed, and we chose 48 h as the incubation time.

As a first step, we ensured that CLL cells could be cultured in 80 nL droplets for 48 h, our planned incubation time. We checked the stability of droplets on DMA for 48 h

in a cell culture incubator and showed that droplets of culture medium on DMA are stable for at least 48 h (**Suppl. Fig. S6**). The viability of cells cultured in 80 nL droplets ranged from 60% to 85% and resembled the viability of cells cultured in T25 cell culture flasks (**Fig. 1c**). We have checked the uniformity of manual plating and viability of cells in individual droplets (**Suppl. Fig. S7**). The number of cells per droplet after 48 h of culture was on average 140 ± 60 cells/spot and was comparable to the variability of cell number per spot (150 ± 70 cells/spot) obtained after seeding cells cultured in flask for 48 h onto DMA slides (**Suppl. Fig. S7**). This indicates that observed variability in number of cells per spot reflects distribution of cells across the array during the manual seeding procedure and not different conditions in each droplet during culturing. The viability of cells cultured for 48 h was on average $80\% \pm 15\%$ and $87\% \pm 7\%$ on the DMA and in the flask, respectively (**Suppl. Fig. S7**). We observed that numbers of cells and cell viability per spot distributed randomly across the tested array area, indicating that there is no inhomogeneity in plating and culturing conditions across the slide (**Suppl. Fig. S7**). These results are in good agreement with our previous study on distribution of cell number across larger array areas using cell lines.²⁸

DSRT on the DMA Platform Using Manual Setup

As a next step, we carried out the compound treatment of primary CLL cells on polymer DMA slides using a manual setup according to the workflow described in **Table 1**. The cells from five different donors were previously tested with a library of anticancer compounds using a previously published workflow in 384-well plates (**Table 1**) at the University Hospital Heidelberg.⁸ We chose nine anticancer compounds commonly used to treat this cancer (**Suppl. Table S1**) and tested them on the DMA platform.

The compound treatment results are presented in **Figures 2 and 3** and **Supplemental Figure S2**. The dose–responses to the compounds obtained on the polymer DMA slides were compared with dose–responses obtained earlier in 384-well plates. We have observed that for all tested compounds the working concentrations were higher on the polymer DMA slides compared with the 384-well plates: 5 times higher for AZD7762, CAL-101, dasatinib, IPI-145, LGX-818, PCI-32765, and MK-2206; 50 times for doxorubicin; and 200 times for Abt199 (**Figs. 2 and 3, Suppl. Fig. S2**). Despite higher working concentrations, we observed similar dose–response trend for doxorubicin, AZD7762, Abt-199, CAL-101, IPI-145, and LGX-818 (**Fig. 2**). In addition, we could spot the donor-specific response pattern; for example, cells from donor 4 were sensitive to compound AZD7762, while donors 3 and 5 revealed no and a partial response to the same compound, respectively (**Fig. 3**).

These results indicate that a higher working concentration of compounds observed on polymer DMA slides might be a consequence of the partial transfer of compounds into droplets and nonspecific adsorption of compounds on the polymer surface or others, which we have investigated in the next step. Regardless of observed higher working concentrations, calculated the Z' factors for polymer DMA and the manual setup were 0.56, 0.85, and 0.72 for three independent repetitions. As previously defined, a Z factor between 0.5 and 1.0 represents “an excellent assay.”³⁷

Comparison of Cell Responses Using Different Experimental Setups

We hypothesized that the higher effective concentrations of compounds on polymer DMA slides could be due to (1) the partial transfer of compounds into droplets, (2) nonspecific adsorption of compounds on the polymer surface, (3) a different cell response in extremely small culturing volumes of 80 nL, and (4) different readouts used to estimate viability on the DMA platform and 384-well plate (**Table 1**). To test these hypotheses, we chose a simple experimental model where we compared the response of a human T-lymphocyte cell line (Jurkat cells) with a range of concentrations of doxorubicin under different experimental conditions. To precisely control the number of cells and culturing volumes per experiment, we used a noncontact liquid dispenser for dispensing compounds and cells in these experiments.

To test our first hypothesis, we compared the cell response to doxorubicin that had been either preprinted directly into hydrophilic spots prior to cell seeding (reverse method) or first printed onto a glass slide and then added to DMA containing cells by sandwiching (sandwiching method) (**Fig. 4a**). We obtained close dose–response curves using the reverse or sandwiching method (**Fig. 4a, Suppl. Table S6**). These results indicate that the transfer rate of compounds from the glass slide into the droplets was not the reason for higher working concentrations of drugs in the case of the polymer DMA slides, at least regarding doxorubicin.

To test the second potential explanation, we compared the response of Jurkat cells to doxorubicin on a polymer DMA and on a nonpolymer DMA slide. Doxorubicin’s IC50 value on polymer DMA slides coated with gelatin was much higher than that obtained on nonpolymer DMA slides coated with gelatin ($\sim 202.51 \mu\text{M}$ vs $35.2 \mu\text{M}$, respectively) (**Fig. 4b, Suppl. Table S6**). Moreover, the IC50 value on nonpolymer DMA slides without gelatin coating was even lower ($\sim 0.19 \mu\text{M}$) and comparable to the IC50 value of doxorubicin in a 384-well plate ($\sim 0.47 \pm 0.2 \mu\text{M}$) (**Fig. 4b, Suppl. Table S6**). Taken together, we conclude that the higher IC50 values obtained on the polymer DMA slides were caused by nonspecific drug adsorption to the porous polymer and gelatin layer. Such adsorption led to a significant increase in IC50 values and can be avoided by employing nonpolymer DMA slides.

To test our third hypothesis, we compared the response of 100 cells to different concentrations of doxorubicin in volumes ranging from 0.1 to 100 μ L. To cover this range of volumes, we used both a nonpolymer DMA platform and polystyrene microtiter plates (**Suppl. Table S5**). We observed close dose–responses in different volumes on the nonpolymer DMA slides and in microtiter plates, with IC₅₀ values ranging randomly from 0.16 to 0.63 μ M (**Fig. 4c, Suppl. Table S6**). These results indicate that there is no effect of small volumes on cell response to drugs, and that the extremely low culturing volumes we had used were not the reason for higher working concentrations of compounds on polymer DMA slides.

To investigate our fourth hypothesis, we compared the dose–response of Jurkat cells to doxorubicin in 384-well plates using microscopy and luminescence-based readout, which resulted in close dose–responses with both methods, with IC₅₀ values of 0.35 and 0.66 μ M for microscopy and ATP assay, respectively (**Fig. 4d, Suppl. Table S6**). Moreover, we observed no difference in cell response when using 100 or 20,000 cells per well, with IC₅₀ values of 0.66 and 0.53 μ M, respectively (**Fig. 4d, Suppl. Table S6**).

Taken together, the nonspecific adsorption of compounds onto functionalized polymer seems to be the main reason for the increase in the drugs’ working concentrations on the polymer DMA surface (**Fig. 4b**), which proved to be entirely avoidable by substituting polymer DMA slides with nonpolymer ones in the workflow for a manual setup (**Table 1**).

DSRT on DMA Platform Using Automated Setup

As a next step, we tested whether the response of primary CLL cells to nine previously tested anticancer drugs on nonpolymer, noncoated DMA slides is indeed comparable to the cell response in 384-well plates via microscopy and luminescence-based readouts. CLL cells were dispensed directly into hydrophilic 1 mm^2 spots preprinted with various concentrations of anticancer drugs, followed by incubating the cells for 48 h. Staining solution containing calcein AM and PI was then dispensed into the droplets using a noncontact liquid dispenser. The dose–responses and IC₅₀ values of eight drugs on the nonpolymer DMA slides concurred closely with the response observed in a 384-well plate (**Fig. 5, Suppl. Table S7**). The IC₅₀ value of MK-2206 was slightly higher on the DMA platform, compared with the 384-well plate (**Fig. 5, Suppl. Table S7**). We also compared dose–responses and IC₅₀ values obtained in the 384-well plate by using different readouts and different cell numbers. We obtained comparable results by using microscopy and an ATP assay, as well as by using 100 and 20,000 cells in a 384-well plate (**Fig. 5, Suppl. Fig. S3, Suppl. Tables S2 and S7**). We compared the variability of data obtained from experiments treating the primary cells

on both nonpolymer DMA and 384-well plates using a microscopy-based readout and observed no difference between the platforms (**Suppl. Fig. S5**). The calculated Z' factors for nonpolymer DMA were 0.79, 0.53, and 0.65 for three repetitions, compared with a Z' factor of 0.59 for the 384-well plate, indicating a robust experimental setup.

Taking together, our results indicate that we can obtain comparable and reliable results on the DMA platform. In other words, by using primary patient-derived cells on the DMA platform with as few as 100 cells in 100 nL culturing volume, we obtained dose–responses comparable to those obtained in a 384-well plate using 20,000 cells in 30 μ L of culturing volume. We have estimated the time and cost of performing the full protocol for each compound on DMA and 384-well plate (**Suppl. Tables S3 and S4**). Considering that automation for printing compounds and cells on both DMA and 384-well plate is used, the time needed for the protocol is similar between the platforms, with approximately 2 h more in the case of DMA for imaging and image analysis (**Suppl. Table S3**). However, cost estimation shows that the price of experiments for each drug (10 concentrations, 4 replicates) is about 10 euros in the case of DMA and 800 euros in the case of 384-well plate (**Suppl. Table S4**), demonstrating clear advantage of miniaturization.

Conclusions

The present work illustrates how we established a workflow for a highly miniaturized DSRT using the DMA platform. We have demonstrated the promising potential of culturing primary CLL cells isolated from patients in 80 to 100 nL droplets for 48 h with high viability. We showed that by using the DMA platform and only 100 cells and 300 times fewer compounds and reagents, we obtained the same results as if we had employed conventional 384-well plates and 20,000 cells per each well. We have demonstrated our system in 2D, however, as we have previously shown that the DMA platform is compatible with culturing cells in 3D environments by means of scaffolds^{34,35} or by promoting the self-organization of cells.³⁵ The possibility of culturing cells in 3D gives rise to even more physiologically relevant applications using primary patient-derived cells.

We demonstrated the application of manual and automated operation of DMA slides for DSRT, both of which can facilitate various applications. The manual setup requires no liquid handling robotics and can be done in a laboratory lacking automation for low- to middle-throughput screenings. On the other hand, our automated setup is beneficial for experiments requiring higher throughputs or even smaller volumes and cell numbers. All the components of the described system for both manual and automated setup are available commercially, and established protocols can be adopted in different laboratories. We believe that highly miniaturized DSRT on our DMA platform has a

potential to open new opportunities in the field of personalized and precision medicine by enabling tests with minute amount of primary patient-derived materials and reagents that were impossible in state-of-the-art microtiter plates.

Acknowledgments

The authors are grateful to Dr. Dietrich and Professor Zenz (Hospital University of Heidelberg) for providing compounds and CLL cells for the study. The authors are grateful to Dr. Christine Blattner (Institute of Toxicology and Genetics, KIT) for providing the Jurkat cell line. The authors are grateful to the Crossmedia service department at KIT and especially to Amadeus Bramsiepe and Willi Mueller for professional photos of DMA.

Declaration of Conflicting Interests

The authors declared the following potential conflicts of interest with respect to the research, authorship, and/or publication of this article: A.A.P. and P.A.L., in addition to being employed by the Karlsruhe Institute of Technology, are (since March 2018) shareholders of Aquarray GmbH. S.D., T.Z., W.H., M.R., and R.P. declare that there is no conflict of interest regarding the publication of this article.

Ethics Statement

All the experiments were performed in accordance with relevant guidelines and regulations. The human material used in the current study was obtained in accordance with the Ethics Committee Heidelberg (University of Heidelberg, Germany; S-356/2013). Patients who donated tumor material provided written informed consent prior to study. In the current study, the patient information was not revealed and obtained results were used exclusively for comparison purposes between two experimental platforms (DMA and microtiter plates) and were not connected back to data of individual patients.

Funding

The authors received the following financial support for the research, authorship, and/or publication of this article: This research was supported by the ERC starting grant (no. 337077-DropCellArray), ERC-PoC grant (no. DLV-680913-CellScreenChip), and EXIST Forschungstransfer (Aquarray 03EFJBW155).

References

1. GBD 2025 Risk Factors Collaborators. Global, Regional, and National Comparative Risk Assessment of 79 Behavioural, Environmental and Occupational, and Metabolic Risks or Clusters of Risks, 1990–2015: A Systematic Analysis for the Global Burden of Disease Study 2015. *Lancet* **2016**, *388*, 1659–1724.
2. Sawyers, C. Targeted Cancer Therapy. *Nature* **2004**, *432*, 294.
3. Brannon-Peppas, L.; Blanchette, J. O. Nanoparticle and Targeted Systems for Cancer Therapy. *Adv. Drug Deliv. Rev.* **2004**, *56*, 1649–1659.
4. Dougan, M.; Dranoff, G. Immune Therapy for Cancer. *Annu. Rev. Immunol.* **2009**, *27*, 83–117.
5. van 't Veer, L. J.; Bernards, R. Enabling Personalized Cancer Medicine through Analysis of Gene-Expression Patterns. *Nature* **2008**, *452*, 564.
6. Syn, N. L.-X.; Yong, W.-P.; Goh, B.-C.; et al. Evolving Landscape of Tumor Molecular Profiling for Personalized Cancer Therapy: A Comprehensive Review. *Expert Opin. Drug Metab. Toxicol.* **2016**, *12*, 911–922.
7. Hanash, S. Integrated Global Profiling of Cancer. *Nat. Rev. Cancer* **2004**, *4*, 638.
8. Dietrich, S.; Oleś, M.; Lu, J.; et al. Drug-Perturbation-Based Stratification of Blood Cancer. *J. Clin. Invest.* **2018**, *128*, 427–445.
9. Maxson, J. E.; Gotlib, J.; Pollyea, D. A.; et al. Oncogenic CSF3R Mutations in Chronic Neutrophilic Leukemia and Atypical CML. *N. Engl. J. Med.* **2013**, *368*, 1781–1790.
10. Sawyers, C. L. The Cancer Biomarker Problem. *Nature* **2008**, *452*, 548.
11. Andersson, E. I.; Pützer, S.; Yadav, B.; et al. Discovery of Novel Drug Sensitivities in T-PLL by High-Throughput Ex Vivo Drug Testing and Mutation Profiling. *Leukemia* **2017**, *32*, 774.
12. Crystal, A. S.; Shaw, A. T.; Sequist, L. V.; et al. Patient-Derived Models of Acquired Resistance Can Identify Effective Drug Combinations for Cancer. *Science* **2014**, *346*, 1480–1486.
13. Pemovska, T.; Kontro, M.; Yadav, B.; et al. Individualized Systems Medicine Strategy to Tailor Treatments for Patients with Chemorefractory Acute Myeloid Leukemia. *Cancer Discov.* **2013**, *3*, 1416–1429.
14. Saarela, J.; Kulesskiy, E.; Laamanen, K.; et al. A Personalised Medicine Drug Sensitivity and Resistance Testing Platform and Utilisation of Acoustic Droplet Ejection at the Institute for Molecular Medicine Finland. *Synergy* **2014**, *1*, 78.
15. Maxson, J. E.; Abel, M. L.; Wang, J.; et al. Identification and Characterization of Tyrosine Kinase Nonreceptor 2 Mutations in Leukemia through Integration of Kinase Inhibitor Screening and Genomic Analysis. *Cancer Res.* **2016**, *76*, 127–138.
16. Pemovska, T.; Johnson, E.; Kontro, M.; et al. Axitinib Effectively Inhibits BCR-ABL1(T315I) with a Distinct Binding Conformation. *Nature* **2015**, *519*, 102.
17. Lu, D.-Y.; Lu, T.-R.; Wu, H.-Y. Personalized Cancer Therapy: A Perspective. *Int. J. Pharm. Pract. Drug Res.* **2014**, *4*, 108–118.
18. Gustavsson, A.; Olofsson, T. Prediction of Response to Chemotherapy in Acute Leukemia by In Vitro Drug Sensitivity Testing on Leukemic Stem Cells. *Cancer Res.* **1984**, *44*, 4648–4652.
19. Larsson, R.; Fridborg, H.; Kristensen, J.; et al. In Vitro Testing of Chemotherapeutic Drug Combinations in Acute Myelocytic Leukaemia Using the Fluorometric Microculture

Cytotoxicity Assay (FMCA). *Br. J. Cancer* **1993**, *67*, 969–974.

20. Yamada, S.; Hongo, T.; Okada, S.; et al. Clinical Relevance of In Vitro Chemoresistance in Childhood Acute Myeloid Leukemia. *Leukemia* **2001**, *15*, 1892.

21. Iwadate, Y.; Fujimoto, S.; Namba, H.; et al. Promising Survival for Patients with Glioblastoma Multiforme Treated with Individualised Chemotherapy Based on In Vitro Drug Sensitivity Testing. *Br. J. Cancer* **2003**, *89*, 1896–1900.

22. Villman, K.; Blomqvist, C.; Larsson, R.; et al. Predictive Value of In Vitro Assessment of Cytotoxic Drug Activity in Advanced Breast Cancer. *Anti-Cancer Drugs* **2005**, *16*, 609–615.

23. Majumder, B.; Baraneehdaran, U.; Thiagarajan, S.; et al. Predicting Clinical Response to Anticancer Drugs Using an Ex Vivo Platform That Captures Tumour Heterogeneity. *Nat. Commun.* **2015**, *6*, 6169.

24. Frismanas, V.; Dobay, M. P.; Rinaldi, A.; et al. Ex Vivo Drug Response Profiling Detects Recurrent Sensitivity Patterns in Drug-Resistant Acute Lymphoblastic Leukemia. *Blood* **2017**, *129*, e26–e37.

25. Tyner, J. W.; Yang, W. F.; Bankhead, A.; et al. Kinase Pathway Dependence in Primary Human Leukemias Determined by Rapid Inhibitor Screening. *Cancer Res.* **2013**, *73*, 285–296.

26. Yamada, S.; Hongo, T.; Okada, S.; et al. Clinical Relevance of In Vitro Chemoresistance in Childhood Acute Myeloid Leukemia. *Leukemia* **2001**, *15*, 1892–1897.

27. Rajer, M. K. M. Quantitative Analysis of Fine Needle Aspiration Biopsy Samples. *Radiol. Oncol.* **2005**, *39*, 269–272.

28. Popova, A. A.; Demir, K.; Hartanto, T. G.; et al. Droplet-Microarray on Superhydrophobic-Superhydrophilic Patterns for High-Throughput Live Cell Screenings. *RSC Adv.* **2016**, *6*, 38262–38276.

29. Popova, A. A.; Depew, C.; Permana, K. M.; et al. Evaluation of the Droplet-Microarray Platform for High-Throughput Screening of Suspension Cells. *SLAS Technol.* **2016**, *22*, 163–175.

30. Popova, A. A.; Schillo, S. M.; Demir, K.; et al. Droplet-Array (DA) Sandwich Chip: A Versatile Platform for High-Throughput Cell Screening Based on Superhydrophobic–Superhydrophilic Micropatterning. *Adv. Mater.* **2015**, *27*, 5217–5222.

31. Tronser, T.; Popova, A. A.; Jaggy, M.; et al. Droplet Microarray Based on Patterned Superhydrophobic Surfaces Prevents Stem Cell Differentiation and Enables High-Throughput Stem Cell Screening. *Adv. Healthc. Mater.* **2017**, *6*, 1700622.

32. Feng, W.; Li, L.; Ueda, E.; et al. Surface Patterning via Thiol-Yne Click Chemistry: An Extremely Fast and Versatile Approach to Superhydrophilic–Superhydrophobic Micropatterns. *Adv. Mater. Interfaces* **2014**, *1*, 1400269.

33. Popova, A. A.; Demir, K.; Hartanto, T. G.; et al. Droplet-Microarray on Superhydrophobic-Superhydrophilic Patterns for High-Throughput Live Cell Screenings. *RSC Adv.* **2016**, *6*, 38263–38276.

34. Neto, A. I.; Demir, K.; Popova, A. A.; et al. Fabrication of Hydrogel Particles of Defined Shapes Using Superhydrophobic-Hydrophilic Micropatterns. *Adv. Mater.* **2016**, *27*, 7613–7619.

35. Tronser, T.; Demir, K.; Reischl, M.; et al. Droplet Microarray: Miniaturized Platform for Rapid Formation and High-Throughput Screening of Embryoid Bodies. *Lab Chip* **2018**, *18*, 2257–2269.

36. Jogia, G.; Tronser, T.; Popova, A.; et al. Droplet Microarray Based on Superhydrophobic-Superhydrophilic Patterns for Single Cell Analysis. *Microarrays* **2016**, *5*, 28.

37. Zhang, J.-H.; Chung, T. D. Y.; Oldenburg, K. R. A Simple Statistical Parameter for Use in Evaluation and Validation of High Throughput Screening Assays. *J. Biomol. Screen.* **1999**, *4*, 67–73.